Drag Reduction of an Elastic Fish Model

Karl-Magnus W. McLetchie
MIT Ocean Engineering Testing Tank

***Abstract*— Investigations into unsteady fish-like locomotion have shown that it is a highly efficient method of marine propulsion. Recent experimental work argued that the power needed to propel a swimming fish-like body is significantly less than the power need to tow an identical, but non-swimming body. This experimental work to prove drag reduction has involved complex robotic systems with many moving parts and actuation devices. Often, the complexity of these systems overshadows their purpose, which is to understand the interaction between the fluid and the body.**

The purpose of this project is to experimentally obtain drag reduction using the simplest experimental setup possible; a solid urethane rubber fish with a single actuator. This simple model does not allow for precise control of the body movement. However, in nature, there are broad ranges of species that are all able to swim efficiently; and inside each species, each individual has a different size, shape, and swimming style. Therefore to fulfill the goal of the project, it should only be necessary to make a model that looks and moves like an "average" fish. A slight change in the model's form or motion should not drastically change the efficiency results.

We chose to base the physical and kinematic characteristics of the model off of a rainbow trout. Trout are a common laboratory fish, and extensive data on their swimming behavior is available.

The model was tested at a range of different actuation amplitudes and frequencies, with a range of Strouhal numbers between 0.1 and 0.5. The highest efficiencies of 30% for a self-propelled fish were measured at a Strouhal number of 0.2. Drag reduction was not shown, because the hydrodynamic efficiency of the fish was not high enough. However, the results show that by adjusting the swimming parameters of the fish, a wide range of efficiencies can be achieved. These results suggest that efficient fish swimming is a finely tuned process. A series of different, evolving fish models will have to be used to maximize efficiency and show drag reduction.

Fish are more efficient and maneuverable than any existing manmade underwater vehicle. A better understanding of the fluid dynamics of fish swimming combined with the development of new technologies such as artificial muscles will allow for the application of unsteady fish-like propulsion to underwater vehicles.

***Index Terms*— fish swimming, drag-reduction**

I. Introduction

FISH have evolved for millions of years to become expert swimmers. Their body shapes and swimming styles have adapted to suit their respective environments.

An in-depth investigation of fish swimming began in 1936, when Gray proposed his paradox on the swimming efficiency of dolphins. He found that dolphins should not be able to produce enough power to swim as fast as they do, given how much power their muscles should produce. One solution that he proposed to the paradox is that swimming dolphins manipulate the flow around them to reduce their drag [1]. This flow manipulation, known as drag reduction, has been studied extensively because of its potential applications to marine vehicles.

Barrett, at MIT, created a robotic bluefin tuna to investigate the mechanism of drag reduction. He found a drag reduction of 60%, meaning that at optimum swimming parameters, the swimming tuna has 60% less drag than the rigid tuna [2]. His results were not replicated by a second generation robotic tuna, which did not demomstrate any drag reduction. [3].

Work has also been done to argue that Gray's analysis is flawed and that no drag reduction mechanism occurs. Fein found that Gray's estimates of swimming speeds of over 10m/s were inaccurate because they were taken by men on moving ships with stopwatches. These measurements were subject to human error, and it is possible additionally that the dolphins were using the ship's wake to increase their speed. Fein reports that the maximum possible swimming speed of a dolphin is actually 8.3m/s. At this speed a dolphin does not need any drag reduction mechanism [4].

Fish has a similar theory based on thorough drag and speed measurements of five trained bottlenose dolphins. He found that the measured propulsive efficiency of the dolphins (80%) is within physiological limits and found no evidence that any drag reduction mechanism occurs in dolphins [5].

In this paper, the controversial subject of drag reduction is investigated using a simple experimental setup. The setup includes a solid urethane rubber fish, a single actuation motor, and a load cell to measure the thrust and drag of the fish. The fish model was run at different actuation amplitudes and frequencies, and the power input and output were measured. From these results, the efficiency and swimming drag were calculated.

II. Form and Kinematic Selection

This section covers the decision making process involved in choosing the fish model's species, swimming parameters, and elasticity.

A. Species Selection

Before choosing a specific species of fish, the decision had to be made between an undulatory swimmer and a lunate tail swimmer. Lunate tail swimmers such as mackerel and tuna use their large tail as a foil to redirect vortices shed by their bodies. Undulatory swimmers, such as cod, trout, and eels move their bodies in a traveling wave that accelerates the surrounding water. The thrust and efficiency of an undulatory swimmer can be modeled by Lighthill's Large-Amplitude elongated body theory [6]. An undulatory fish was chosen because mimicking a lunate tail swimmer would require precise tail control. Flexible beams can not be precisely controlled, but they

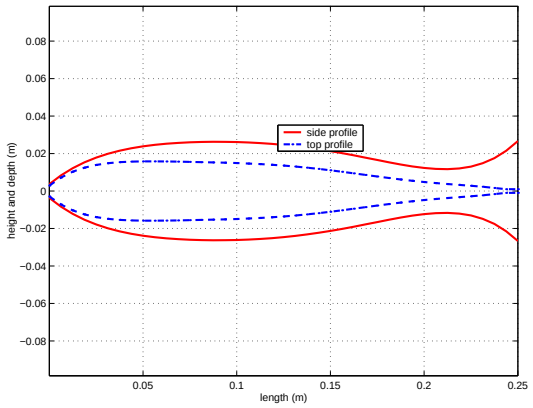

Fig. 1. The curves of a rainbow trout

TABLE I
FISH CHARACTERISTICS

Notation	Value	Description
L	30cm	length
U	1m/s	forward speed
Tbf	6.4Hz	tail beat frequency
Tba	4.5cm	tail beat amplitude(total)
λ	23cm	body wavelength
c	1.45 m/s	body wavespeed
Re	$3x10^5$	Reynolds number (based on length)
St	0.28	Strouhal number

naturally create traveling waves that can generate propulsive forces.

Rainbow trout, *salvelinus fontinalis*, were chosen because they are an undulatory swimming fish that have been studied extensively. To get the form of the fish model, a dead rainbow trout was photographed, and the outline was curve fit. The top and bottom curves, shown in Figure 1, were averaged to make symmetric profiles. In a 3-D Cad program, an ellipse was swept along these curves to create a 3-D model of the fish. This model was used in the design of the mold.

B. The Rainbow Trout

In his analysis of Rainbow Trout, Webb measured their swimming parameters as shown Table 1 [7].

Based on Lauder's analysis of trout and bass [8] the amplitude of motion should vary as as:

$$z(x,t) = A(x - x_\circ)^2 \sin(kx - \omega t) \quad (1)$$

Where A is a constant that gives the correct tail beat amplitude, and $x_\circ$, is the actuation point (point of no lateral motion). $x_\circ$ should be at 28% of the body length from the head.

C. Numerical Work

To predict the behavior of the rubber model and match the elasticity modulus of the rubber with the correct body amplitude and wave speed, a numerical program was used. This program solved the Bernoulli-Euler beam equation with a varying cross section, added mass, viscous damping, forward speed effects, and an imposed actuation angle at $x_\circ$.

The program determined that to obtain the desired body wave speed of 1.4 m/s (Section II-B) a rubber with a modulus of elasticity of $1.5x10^5$ Pa had to be used. Evergreen-10, a two-part urethane rubber available from Smooth-On (Easton, Pa), has this modulus of elasticity, and was used to cast the fish.

III. EXPERIMENTAL APPARATUS AND METHODS

In this section, the mechanical and electronic design of the apparatus are covered, along with the methods of data collection.

All of the tests were run in the MIT Ocean Engineering Testing Tank, a 30m long, 2.5m wide, 1.2m deep rectangular testing tank. The main towing carriage was used to tow the experimental apparatus at a constant velocity of 1 m/s.

A. Fish Construction

The exact shape of the fish was taken from a real trout, and the casting material was chosen to give the fish the correct wave speed.

A 0.635 cm (1/4 inch) stainless shaft was used to connect the motor shaft to the fish. This shaft was bolted to the 1.6mm thick polyethylene skeleton, which was designed to add stiffness to the tail without significantly changing the dynamics of the rest of the body.

To cast the fish, the EV-10 two-part urethane was poured into a mold around the shaft and skeleton.

B. Carriage Mount

Figure 2 shows a three dimensional picture of the apparatus. Figure 3 in Section III-C shows a simpler profile view of the apparatus. The carriage mount was designed in a 3-D CAD program and machined to within 0.2mm of accuracy. It is composed of a main aluminum frame, which holds the motor and force sensor, an aluminum mast (Hall Spars, Bristol, RI), which runs down to the fish, and low friction teflon bearings. The bearings mount the frame to a mounting plate which bolts to the towing tank carriage. Note that the drive shaft runs through a bearing in the motor, at the top of the mast, and at the bottom of the mast. This keeps the shaft aligned properly and free of vibration.

C. Force and Moment Balance

Figure 3 a) shows all of the external forces acting on the system and the lengths of all of the moment arms. Figure 3 b) shows the same system, but with the fish removed. Definitions of the variables used are given in Table 2. For all force measurements, the sensor force, F_s, was recorded and a moment balance around the bearing was calculated.

The mast drag, D_m, is constant because the towing velocity of $U = 1m/s$ is kept constant for all of the runs. To measure D_m, the fish was taken off the mast, and the blunt end was rounded over to reduce end-effects. During repeated runs, a mast drag of $0.58N$ was measured, acting at the center of the submerged length of mast, L_m. The mast drag is accounted for in all fish force calculations.

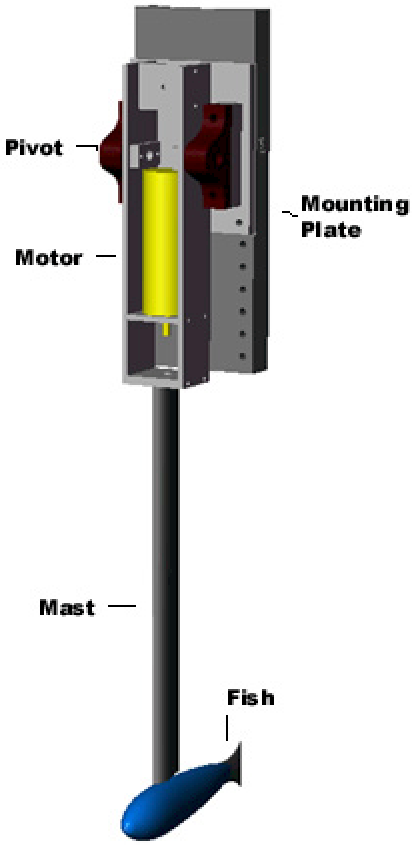

Fig. 2. Experimental Setup

The drag of the unactuated fish, D_r, is needed for the power-output and drag reduction calculations. To measured D_r, the fish was reattached to the mast, and run down the tank with no actuation. An unactuated drag of $0.175N$ was measured, acting along the centerline of the fish.

The measured drag of the mast and unactuated fish compared favorably to Hoerner's measurements of foils and streamlined bodies [9].

The drag and the thrust of the of the swimming fish can not be independantly measured because they act at the same distance from the bearing, L_F. For simplification, the swimming drag and thrust are combined into one force, F_m, which represents the force that the mast exerts on the fish.

$$F_m = T - D \tag{2}$$

D. Electronics and Data Collection

The two main electronic systems involved in this experiment are the servo system, which drives the fish, and the load cell system, which measures the longitudinal force on the fish. Signals from these systems are recorded by a data acquisition computer and filtered with a Butterworth filter that took out all signal noise above 20Hz.

The servo system is composed of the servo motor and its amp and transformer. The motor used is a Pittman (Pittman, Harleysville, PA) 14000 24 V DC motor. The motor is gearless to prevent backlash and reduce friction losses. The motor encoder is an optical 500 count quadrature encoder, meaning that it can determine direction and uses 2000 encoder counts to define a full rotation. The motor is controlled by a motion control card, which takes in position commands from the user and outputs the actual position and commanded torque to the data acquisition computer. These signals are used for the power input calculation.

TABLE II
DESCRIPTION OF VARIABLES FROM FIGURE 3. LENGTHS ARE TAKEN FROM THE ZERO POINT AT THE BEARING.

Variable	Description	Length variable	length value (m)
F_s	sensor force	L_s	0.076
F_B	bearing force		0.000
D_m	mast drag	L_m	0.398
D	fish drag	L_F	0.544
T	fish thrust	L_F	0.544
F_m	force of mast	L_F	0.544

The load cell used was an Entran (Entran Devices, Fairfeild, NJ) dynamic, tension-compression load cell. It has a linear range of $\pm 44N$. It requires a 5V excitation voltage and returns a full scale response of 166mV. To amplify this response, an Ectron adjustable amplifier was used with a gain of 50x. This amplified force signal was recorded by the data acquisition computer and used in the power output calculation.

E. Power Input

The power input to the fish, P_{in}, comes from the servo motor and carriage motor. The carriage motor only supplies power if the fish's thrust does not overcome its drag (F_m is negative). These non self propelled cases are ignored in the final efficiency results.

The power input for self propelled or better cases was calculated by multiplying the torque signal, τ, by the time derivative of the position signal, $\dot{\theta}$. The torque signal was measured by sampling the torque commanded by the MEI motion control card, and the angular position signal was measured by sampling the motor encoder counts.

Figure 4 shows 0.4s of the 20s long torque and position signals. The top graph in Figure 4 is a graph of θ. The motor was commanded to follow a sinusoidal amplitude path, and the data shows that it follows the path closely. The following expressions approximate the data, which is shown in the figures.

$$\theta = A_\theta \sin \omega t \tag{3}$$

Where A_θ is the amplitude of the position signal (13° or 0.23 rad) and ω is actuation frequency (8 Hz or 50.2 rad/s). The second graph in Figure 4 is a graph of the time derivative of the position, $\dot{\theta}$, which was calculated by numerically taking the slope between each data point.

$$\dot{\theta} = \omega A_\theta \cos \omega t \tag{4}$$

The third graph in Figure 4 shows the torque signal, τ

$$\tau = A_\tau \cos \omega t \tag{5}$$

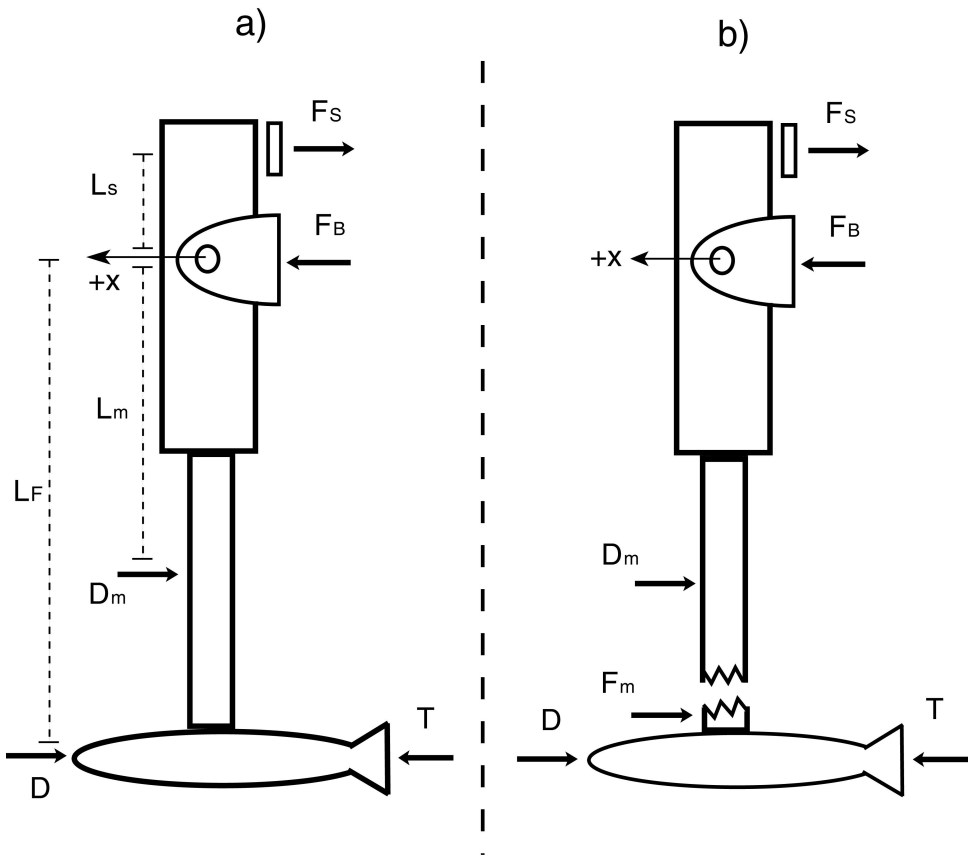

Fig. 3. Diagram of all forces on the system.

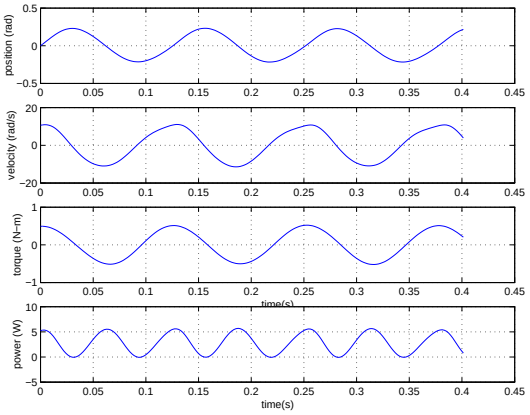

Fig. 4. The drive shaft's angular postition, angular velocity, torque, and power.

Finally, the fourth graph in Figure 4 shows P_{in}.

$$P_{in} = \tau * \dot{\theta} = A_\theta A_\tau \omega \cos^2 \omega t \tag{6}$$

The time averaged power, $\bar{P_{in}}$, is used for all future calculations as the input power by the driving motor.

F. Power Output

The useful power output by the fish was computed by multiplying the net thrust force, $\triangle F$, by the forward velocity, U.

$$P_{out} = \triangle F * U \tag{7}$$

Where $\triangle F$ is the net force produced by the fish.

$$\triangle F = F_m + D \tag{8}$$

D, the fish's drag, can be represented by D_s or D_r depending on the situation. The power output of the fish is calculated by multiplying $\triangle F$ by the forward velocity, where:

$$\triangle F = F_m + D_r \tag{9}$$

D_r was used instead of D_s because D_s can not be measured.

IV. Results

This section presents the power input, mast force, power output, efficiency, and drag reduction results. These results were taken at actuation amplitudes ranging from 7° to 15° and actuation frequencies ranging from 3.5 Hz to 8 Hz. The results were shown to be repeatable and to have an error of less than 10%

A. Power Input

Figure 5 shows the power input curves for the ranges of actuation amplitudes and frequencies. The power required to drive the fish increases with amplitude and frequency.

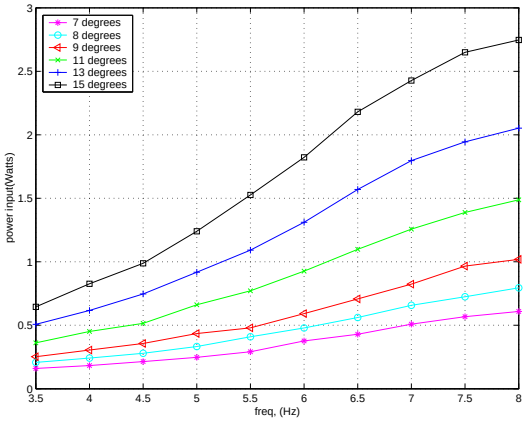

Fig. 5. Power-in measurements for runs of different frequency and amplitude. Power input is measured from the actuation motor current

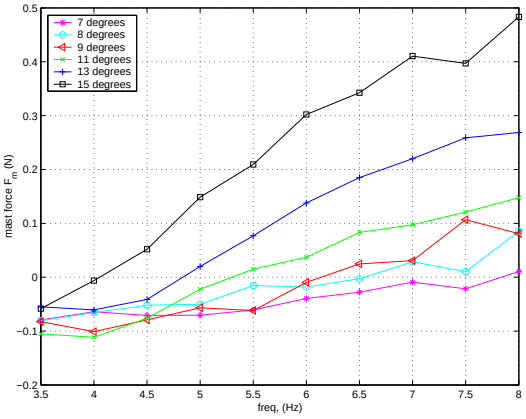

Fig. 6. F_m, the force the the mast exerts on the fish. At $F_m = 0$ the fish is self propelled.

B. Mast Force and Power Output

Figure 6 shows a plot of the mast force, F_m, for all runs. If F_m is greater than zero, then the fish is producing excess thrust, and if F_m is less than zero, then the fish is producing insufficient thrust. All of the amplitudes used Figure 6 produce excess thrust, at some frequency.

Figure 7 shows the P_{out} for all runs. It is the same as the of mast force Figure 6 except it is shifted upwards by D_r and multiplied by U=1m/s.

C. Efficiency

The Efficiency of the fish, η, is defined as the power output divided by the power input.

$$\eta = \frac{P_{out}}{P_{in}} \tag{10}$$

Figure 8 and Figure 9 show the efficiencies measured for all runs of the fish. Many of the values at low frequencies and amplitudes are large because the carriage is adding power to the system.

To limit the results to thrust producing cases, Figure 10 shows cases where $T \geq D_r$. The plot shows the best efficiencies at low actuation amplitudes and at frequencies that approach the design frequency of the fish (6.5 Hz). There

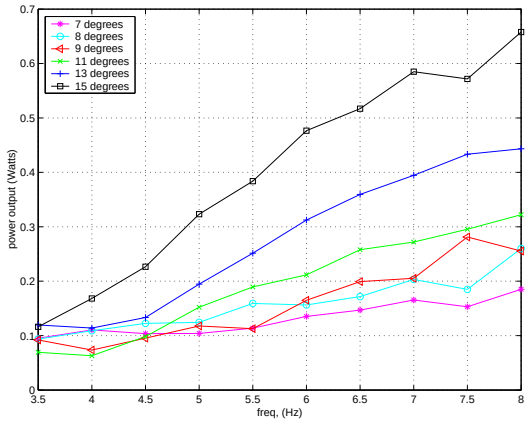

Fig. 7. The power output of the fish. This graph is simply Figure 6 shifted upwards by $D_r = 0.175N$, and multiplied by U=1m/s.

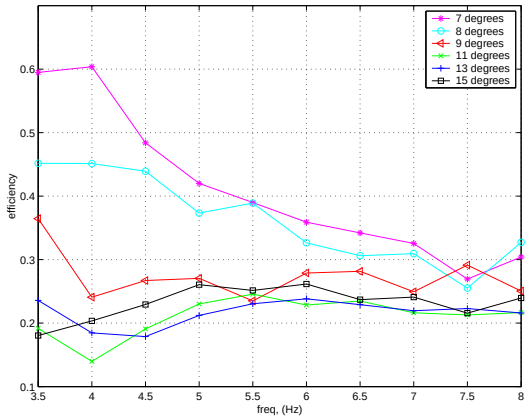

Fig. 8. The efficiency of the fish. The large values at low frequencies are cases where the fish is not self propelled.

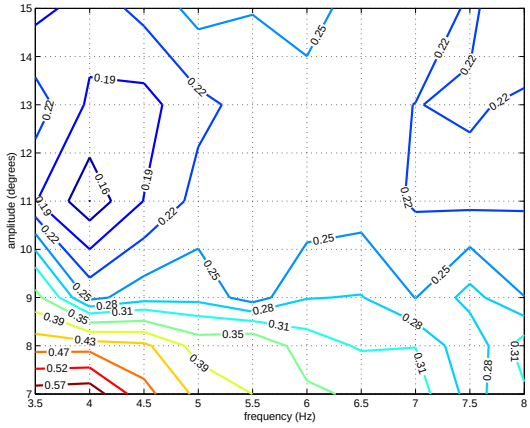

Fig. 9. Contour plot of efficiencies for all tests.

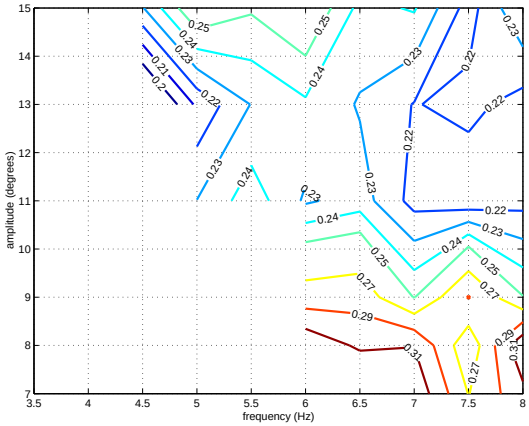

Fig. 10. Contour plot of efficiencies for thrust producing tests.

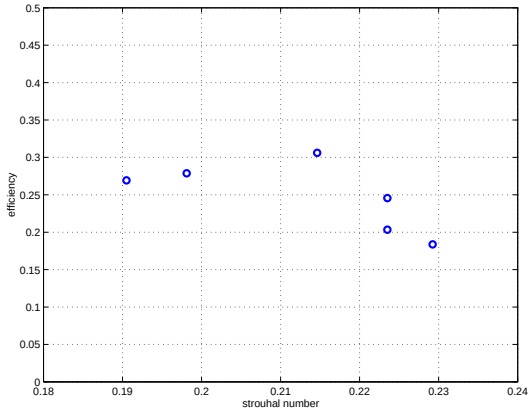

Fig. 11. Efficiencies for self-propelled fish at a rough estimate of Strouhal number

is also an increase in efficiency at low amplitudes and high frequencies that could be due to an erroneous data point, or could indicate that more tests at higher frequencies should be performed.

Figure 11 shows efficiency verses Strouhal number, St, for self-propelled cases. This plot shows a peak efficiency somewhere between Strouhal number 0.2 and 0.22. The fish was designed to run at a Strouhal number of 0.29.

$$St = \frac{f * tba}{U} \tag{11}$$

The tail beat amplitude, tba, or total excursion of the tail, cannot be calculated from the actuation amplitude because the body is flexible. To make a rough measurement of tba, the fish tail was observed on video with a ruler as reference and the tail excursion was recorded. This measurement is rough, but it gives a good estimate of the Strouhal number, so that the results can be compared to previous work.

D. Drag Reduction

Drag reduction occurs if the swimming drag, D_s is less than the rigid drag, D_r.

$$D_s < D_r \tag{12}$$

Calculating drag reduction involves comparing the drag of a swimming fish, D_s, with the drag of a rigid fish, D_r. When

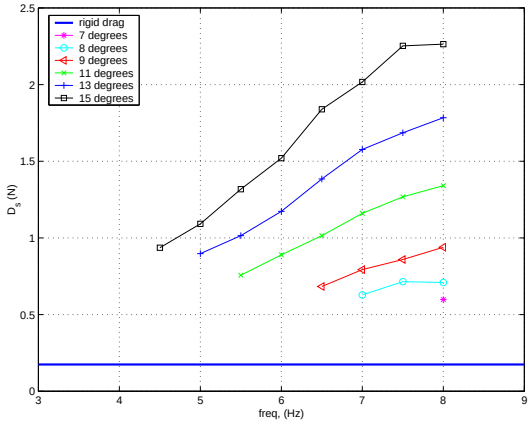

Fig. 12. Upper bound estimate of D_S.

a dead or rigid fish is towed through the water at a constant velocity, the force needed to tow it equals D_r. A live fish, swimming, produces a thrust force, which equals D_s while the fish is swimming at a constant velocity. If drag reduction occurs, then $D_s < D_r$. D_s can not be measured directly because it can not be separated from the thrust force. To prove drag reduction, we must find an upper bound estimate of D_s and compare it to D_r. By measuring the power input, P_{in}, and the forward velocity, U, the upper bound of D_s can be estimated [2].

Rigid drag was measured as D_r=0.175N. The upper bound of D_s is measured using the power-in and the mast force.

$$P_{in} = P_L + P_W + P_{out} \tag{13}$$

Where P_L represents the transmission losses in the motor and bearings, and P_W represents the energy lost in the wake of the fish. P_L should be small because the apparatus uses a gearless motor and low friction bearings. P_W is the power lost to the fluid that should be minimized if the fish was designed to swim efficiently.

Because P_L and P_W are both positive quantities.

$$P_{out} < P_{in} \tag{14}$$

and

$$P_{out} = (F_m + D_s) * U \tag{15}$$

so

$$D_s < \frac{P_{in}}{U} - F_m \tag{16}$$

and the upper bound for D_s is

$$D_s = \frac{P_{in}}{U} - F_m \tag{17}$$

Figure 12 shows the upper bound of D_s for runs in which the fish is self-propelled or producing thrust. D_s is not less than D_r for any of the runs, so drag reduction cannot be proved.

V. Conclusions

The purpose of this project was to make a simple model of a fish to measure how efficiency varies with swimming parameters, and to investigate drag reduction.

The efficiency results showed maximum efficiencies, for a thrust producing fish, of 30% at low actuation amplitudes and at frequencies around the design frequency of 6.5Hz. The division of errors in these results leads to a large error at low actuation amplitudes and frequencies. The frequency of 6.5Hz is large enough to limit the range of the maximum efficiency to $30\% \pm 10\%$.

The results of the drag reduction analysis are inconclusive, because drag reduction is never proved. The estimate of the swimming drag was an upper bound estimate. It would only be close to the actual swimming drag value (and low enough to prove drag reduction) if the fish demonstrated high mechanical and propulsive efficiency. The mechanical efficiency should have been very high because the servo motor used was gearless and the bearings were frictionless. No other mechanical power losses were present in the system. For future experiments, these mechanical power losses should be measured, to ensure that they are small and to improve the results of the drag reduction analysis.

Assuming that the mechanical power losses are small, the majority of the power must have been lost into the wake. The efficiency never exceeded 32% for the self-propelled fish. To prove drag reduction, this efficiency would have to be above 100%.

Although these high efficiencies were not achieved, the results are still promising because they show that efficient fish swimming is a finely tuned process. The thrust and efficiency of the fish were highly dependent on the chosen swimming parameters. It is likely that this initial, simple experiment did not use the ideal body shape, flexibility, actuation amplitudes, or actuation frequencies. A series of different, evolving fish models may be able to maximize efficiency and show drag reduction.

ACKNOWLEDGMENT

The author would like to thank Professor D. Yue, Professor M. Triantafyllou, and Dr. F. Hover for their support and guidance. He would also like to thank the students of the Towing Tank for their help.

REFERENCES

[1] J. Gray, "Studies of animal locomotion vi," *Journal of Experimental Biology*, vol. 13, pp. 192–199, 1936.
[2] D. Barrett, M. Triantafyllou, M. G. D. Yue, and M. Wolfgang, "Drag reduction in fish-like locomotion," *Journal of Fluid Mechanics*, 1999.
[3] D. Beal, "Personal reference," May 2002, from principle researcher.
[4] J. Fein, "Dolphin drag reduction:myth or magic," *Proc. Int. Symp on Seawater Drag Reduction*, 1998.
[5] F. Fish, "Power output and propulsive efficiency of swimming bottlenose dolphins," *Journal of Experimental Biology*, vol. 185, pp. 179–193, 1993.
[6] J.Videler, *Fish Swimming*. London: Chapman and Hall, 1992.
[7] P. Webb and P. Kostecki, "The effect of size and swimming speed on locomotor kinematics of rainbow trout," *Journal of Experimental Biology*, vol. 109, pp. 77–95, 1984.
[8] G. Lauder and B. Jayne, "Speed effects on midline kinematics during steady undulatory swimming of largemouth bass," *The Journal of Experimental Biology*, no. 198, pp. 585–602, 1995.
[9] S. Hoerner, *Fluid-Dynamic Drag*. Vancouver, Washington: Hoerner Fluid Dynamics, 1965.